Applied Thermal Engineering 113 (2017) 1290–1302

Contents lists available at ScienceDirect

Applied Thermal Engineering

journal homepage: www.elsevier.com/locate/apthermeng

Research Paper

Prediction models and control algorithms for predictive applications of setback temperature in cooling systems

Jin Woo Moon [a], Younju Yoon [b], Young-Hoon Jeon [a], Sooyoung Kim [c,*]

[a] School of Architecture and Building Science, Chung-Ang University, Seoul, South Korea
[b] Samsung C&T Corporation, Construction Technology Center, Seoul, South Korea
[c] Department of Interior Architecture & Built Environment, Yonsei University, Seoul, South Korea

HIGHLIGHTS

- Initial ANN model was developed for predicting the time to the setback temperature.
- Initial model was optimized for producing accurate output.
- Optimized model proved its prediction accuracy.
- ANN-based algorithms were developed and tested their performance.
- ANN-based algorithms presented superior thermal comfort or energy efficiency.

ARTICLE INFO

Article history:
Received 6 July 2016
Revised 5 October 2016
Accepted 12 November 2016
Available online 14 November 2016

Keywords:
Temperature control algorithm
Setback temperature
Cooling system
Artificial neural network
Prediction model
Optimization
Thermal conditioning

ABSTRACT

In this study, a temperature control algorithm was developed to apply a setback temperature predictively for the cooling system of a residential building during occupied periods by residents. An artificial neural network (ANN) model was developed to determine the required time for increasing the current indoor temperature to the setback temperature. This study involved three phases: development of the initial ANN-based prediction model, optimization and testing of the initial model, and development and testing of three control algorithms.

The development and performance testing of the model and algorithm were conducted using TRNSYS and MATLAB. Through the development and optimization process, the final ANN model employed indoor temperature and the temperature difference between the current and target setback temperature as two input neurons. The optimal number of hidden layers, number of neurons, learning rate, and moment were determined to be 4, 9, 0.6, and 0.9, respectively. The tangent–sigmoid and pure-linear transfer function was used in the hidden and output neurons, respectively. The ANN model used 100 training data sets with sliding-window method for data management. Levenberg-Marquart training method was employed for model training. The optimized model had a prediction accuracy of 0.9097 root mean square errors when compared with the simulated results.

Employing the ANN model, ANN-based algorithms maintained indoor temperatures better within target ranges. Compared to the conventional algorithm, the ANN-based algorithms reduced the duration of time, in which the indoor temperature was out of the targeted temperature range, as much as 56 and 75 min, respectively. In addition, two ANN-based algorithms removed less heat from indoor space as much as 1.06% and 1.26%. Thus, the applicability of the ANN model and the algorithm presented their potential to be applied for more effective thermal conditioning with reduced energy consumption.

1. Introduction

Thermal conditioning system generally consumes a substantial amount of energy in buildings. In Korea, the energy consumed by the system accounts for 58.1% and 29.6% of the total energy consumption in residential buildings and all buildings, respectively [1,2]. Various theoretical and practical approaches for efficient

* Corresponding author.
E-mail addresses: gilerbert73@cau.ac.kr (J.W. Moon), younju.yoon@samsung.com (Y. Yoon), jeonyh@cau.ac.kr (Y.-H. Jeon), sooyoung@yonsei.ac.kr (S. Kim).

http://dx.doi.org/10.1016/j.applthermaleng.2016.11.087
1359-4311/

Nomenclature

$TEMP_{IN}$	indoor air temperature [°C]	M_i	numerically simulated values by MATLAB and TRANSYS
$\Delta TEMP_{IN}$	change in indoor air temperature from the preceding control cycle [°C]	N_{HL}	number of hidden layers
$TEMP_{OUT}$	outdoor air temperature [°C]	N_{HN}	number of hidden neurons
$\Delta TEMP_{OUT}$	change in outdoor air temperature from that 1 h earlier [°C]	LR	learning rate
$TEMP_{DIF}$	difference between the current and setback temperature [°C]	MO	momentum
$TIMP_{CUR}$	current time	w	connection weight
$TIMP_{SBT}$	predicted time required for increasing the current indoor temperature to the setback temperature, min	NET	summation function
S_i	values predicted by ANN models	TF	transfer function
		o_{pj}	output from the hidden neurons
		o_{pk}	output from the output neurons
		t_{pk}	desired output

energy conservation and maintaining comfortable indoor thermal environments have been examined [2–9]. The application of a setback temperature in residential thermal conditioning systems during nighttime and unoccupied daytime periods is a widely adopted example of such methods.

Appropriate setback temperature application can save up to 23% and 53% of the energy consumption for cooling and heating, respectively [2–9]. In particular, nighttime and daytime setback application can conserve up to 16.9% and 53.0% of the energy consumption for cooling and heating in regions with a hot and humid climate as well as 9.5% and 28.2% of the energy consumption for cooling and heating in regions with a cold climate [2].

Apart from energy conservation, maintaining the thermal comfort of the occupants is a crucial factor relevant to the indoor environmental quality in residential buildings. For example, early setback application can improve energy efficiency but can also lead to thermal discomfort. Thus, the optimal onset time of the setback temperature must be determined under constraints of both thermal comfort and energy efficiency.

Artificial neural networks (ANNs), which is a type of artificial intelligence, have high potential as an advanced strategy for controlling indoor thermal conditions and realizing high building energy efficiency. McCulloch and Pitts developed a computational ANN model that replicates the biological and learning processes of human neural systems [10]. ANN models comprise three layers: input, hidden, and output layers. The input layer uses a series of neurons as the input, and the hidden layers are comprised of hidden neurons. The output layer employs numerous output neurons.

Neurons between in different layers are connected according to their specific weights, and the neurons in the hidden layers and the output layer have transfer functions. ANN models involve two major processes. The first process is the feed forward process for calculating the output from a series of inputs. This process uses the connectivity (i.e., weights, w) between the neurons and the transfer functions. The output of an ANN model makes predictive controls feasible. For example, each input value is multiplied by its own weight between the input and hidden neurons. Values arrived at each hidden neuron are summed by the neurons in the hidden layer. The hidden neurons produce new values by using their transfer function, which are weighted and forwarded to the output neurons. Similarly, the output neurons sum the values and generate outputs by using their transfer function.

The second process is back-propagation for self-learning by using the output error, which is the difference between the calculated and desired outputs. This iterative self-learning process continuously updates the connectivity between the neurons, thus realizing adaptive control [11].

ANN model–based controls are superior to mathematical models, such as regression models or proportional–integral–derivative (PID) controllers, in terms of predicting and controlling the accuracy of thermal loads and systems operation in buildings. ANN-based control strategies can provide better thermal conditions and improved building energy efficiency. The outcomes of relevant studies are summarized in Table 1.

In particular, a method was studied to determine the optimal start moment of the setback period for the heating system [25]. In the study, an artificial neural network (ANN) model was developed for predicting the required time duration from the current indoor temperature to drop the designated setback temperature for the heating system. Five input variables were initially employed as input neurons – indoor air temperature, change from the indoor air temperature of the preceding control cycle, outdoor air temperature, change of the outdoor air temperature from one hour prior, and temperature difference from the setback temperature. After optimization of the ANN model for the input neuron selection, number of hidden layer and neurons, learning rate, and moment, the optimized model showed statistically meaningful prediction accuracy.

Along with the space heating, the space cooling is also a key factor in creating comfortable indoor thermal environments. Although relevant studies have yielded useful findings for the heating systems, the optimal method for controlling the cooling systems has not been comprehensively investigated. In other words, a control strategy for realizing improved thermal environments at high energy efficiency is lacking.

Therefore, this study focuses on two research objectives. The primary objective is to develop an ANN-based prediction model to determine the optimal onset time of the setback temperature during normal occupied periods in a building in cooling seasons. The secondary objective is to develop a control algorithm by using the prediction model to create better thermal environment in space with low energy consumption. The optimal onset of setback temperature would save avoidable energy consumption and provide thermal environments that are within a target range during the early part of the unoccupied periods.

To achieve these objectives, the study is divided into three major phases, as illustrated in Fig. 1. First, an initial prediction model was developed using the ANN theory. In addition, the relationship between the input and output variables were statistically analyzed, and the final input variables for the ANN model were determined through this analysis.

Second, the model was optimized by parametrically examining the performance of the ANN model with variation in the number of hidden layers (N_{HL}), the number of hidden neurons in each hidden

Table 1
Previous studies using the ANN models.

Reference number	Author(s)	Objectives and findings
[12,13]	Mohanraj et al.	• Review of ANN applications for thermal analysis of heat exchangers using four categories, (i) modeling, (ii) parameter estimation, (iii) phase change characteristics estimation, and (iv) controlling • Review of ANN applications for energy and exergy analysis of refrigeration, air conditioning and heat pump systems
[14,15]	Mba et al.; Papantoniou and Kolokotsa	• ANN models for predicting indoor and outdoor thermal conditions such as indoor temperature and humidity as well as outdoor temperature • Proving strong correlation results between the ANN predictions and the experimental/measured data
[16–20]	Deb et al.; Chae et al.; Li et al.; Paudel et al.; Escrivá-Escrivá et al.	• ANN models for forecasting load and energy for building thermal conditioning • Presentation of accurate predictability for the load and energy consumption, thus potential to work as fundamental determinants for controlling building thermal conditions more comfortably and energy-efficiently
[11,21]	Moon et al.	• ANN models for controlling indoor temperature, humidity, and PMV of residential buildings • Provision of more stable and comfortable thermal conditions • Provision of similar amount of energy by ANN applications compared to the non-applications of ANN
[22–25]	Yeo and Kim KW; Yang and Kim; Moon and Jung	• ANN models and algorithms for predicting and employing the optimal start and stop moment of the setback period for the heating system in the office buildings as well as accommodation buildings • Presentation of prediction accuracy and applicability of the ANN models • Potential to operate more comfortable and energy-efficient thermal controls by ANN-based algorithms
[26–30]	Moon et al.	• ANN models for optimally controlling the openings of the double skin envelopes and thermal control systems • Provision of more comfortable thermal environment in double skin buildings
[31–35]	Argiriou et al.; Morel et al.; Lee et al.	• ANN models for operating hydronic heating systems of solar buildings, radiant heating system, and radiant underfloor heating system • Reduction of heating energy consumption and provision of more stable and comfortable thermal environment
[36]	Yaïci and Entchev	• ANN models for predicting the performance of a solar thermal energy systems used of domestic hot water and space heating • Provision of high accuracy and reliability for predicting the preheat tank stratification temperatures and solar fraction
[37]	Chow et al.	• Incorporative method using ANN and Genetic algorithm for the optimal use of fuel and electricity for operating an absorption chiller system • Presentation of prediction accuracy for the mass flow rated of diesel oil, electric power of the cooling water pump, chilled water pump, and coefficient of performance (COP) of the system
[38–40]	Esen et al.	• ANN models for operating ground coupled heat pump system (GCHP) • Applicability with accurate prediction results for the coefficient of performance (COP) of ground coupled heat pump (GCHP) system
[41]	Fannou et al.	• ANN model for predicting the compressor power consumption and heating capacity of the direct expansion geothermal heat pump • Providing very satisfactory prediction accuracy for target outputs

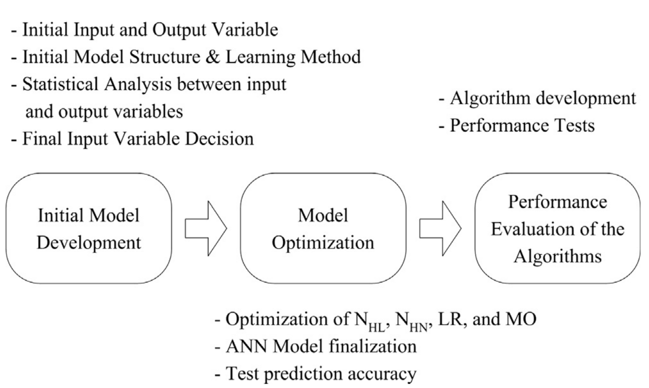

Fig. 1. Research process.

layer (N_{HN}), the learning rate (LR), and the moment (MO). The optimal values were applied to the initial model, and its prediction performance was analyzed.

Finally, the control algorithm employing the optimized ANN model was developed. The control performance of two ANN-based predictive algorithms and a conventional algorithm were comparatively examined in terms of thermal quality and energy efficiency in order to demonstrate the potential and applicability of the proposed algorithm.

2. Initial model development and optimization

2.1. Initial model

An ANN-based model was designed to calculate the time ($TIMP_{SBT}$) required for increasing the current indoor temperature to the setback temperature. The obtained $TIMP_{SBT}$ was subsequently used in the control algorithm for employing the setback temperature prior to the beginning of the unoccupied period. For example, at a current temperature of 24.0 °C, the target setback temperature is 28.0 °C, and $TIME_{SBT}$ is the amount of time in minutes to increase of the temperature from 24.0 °C to 28.0 °C. If the sum of $TIMP_{SBT}$ and the current time is at or after the beginning of the unoccupied period, the algorithm employs the setback temperature at this moment before the actual unoccupied period.

Fig. 2 depicts the initial model. The initial layer was composed of five input neurons: indoor air temperature ($TEMP_{IN}$, °C), change in indoor air temperature from the preceding control cycle ($\Delta TEMP_{IN}$, °C), outdoor air temperature ($TEMP_{OUT}$, °C), change in outdoor air temperature from that 1 h earlier ($\Delta TEMP_{OUT}$, °C), and difference between the current and setback temperatures ($TEMP_{DIF}$, °C). The initial input neurons were selected since they were relevant to the output neuron, which is the predicted time required for increasing the current indoor temperature to the setback temperature ($TIMP_{SBT}$, min). The final input neuron was determined through the statistical analysis using linear correlations between the initial input neurons (namely, $TEMP_{IN}$, $\Delta TEMP_{IN}$,

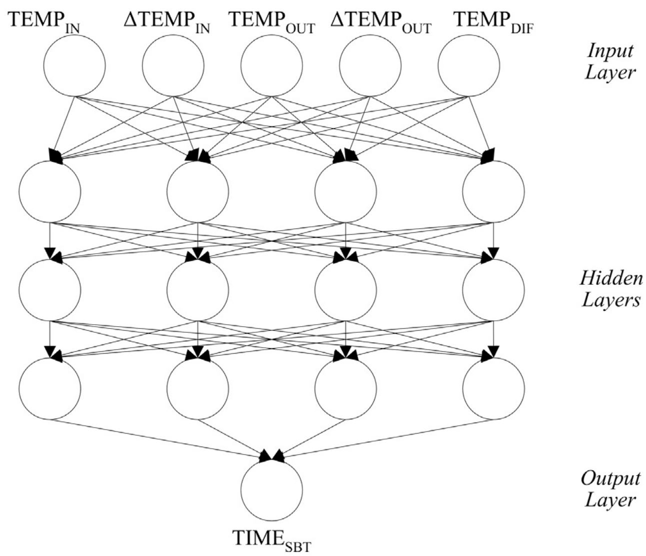

Fig. 2. Initial ANN model.

$TEMP_{OUT}$, $\Delta TEMP_{OUT}$, and $TEMP_{DIF}$) and the output neuron (namely, $TIME_{SBT}$). The neurons which had strong correlation were employed as the final input neurons.

The input values for each neuron were normalized to be between 0 and 1 before being multiplied by its weight. The ranges for $TEMP_{IN}$, $\Delta TEMP_{IN}$, $TEMP_{OUT}$, $\Delta TEMP_{OUT}$, and $TEMP_{DIF}$ were 10 °C to 30 °C, −10 °C to 10 °C, −20 °C to 40 °C, −10 °C to 10 °C, and 0 °C to 10 °C, respectively. The ranges of input neuron covered the normally occurred conditions in Korea.

The number of hidden layers (N_{HL}) and the number of neurons in each hidden layer (N_{HN}) were initially assigned as 3 and 4, respectively based on the models in a previous study which developed an ANN model for predicting a time required for changing from the current temperature to the set-point temperature of the cooling system in accommodation building [42]. The optimal number of hidden layer and hidden neuron were finalized through the optimization process described in Section 2.2. The tangent–sigmoid transfer function was used in the hidden neurons. In addition, an output ($TIME_{SBT}$) and pure linear transfer functions were employed in the output neuron.

For model training, 100 training data sets were prepared. MATLAB (matrix laboratory) [43] and TRNSYS (transient systems simulation) [44] software were used to acquire the data sets for training ANN model. Fig. 3 illustrates the incorporative data collection process for developing the ANN model and the performance testing of the algorithm.

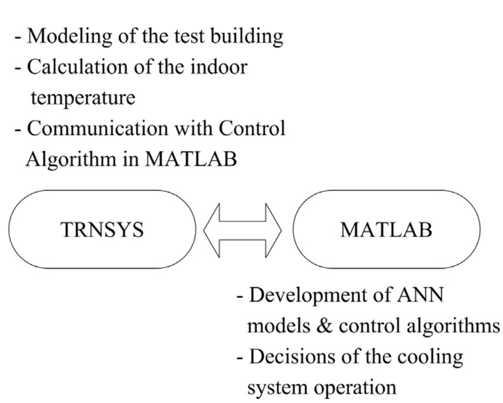

Fig. 3. Cooperation of TRNSYS and MATLAB adopted in the study.

Table 2 describes component types, roles and the modeling results obtained using TRNSYS and MATLAB. The TRNSYS software was employed for modeling the test building and calculating its indoor temperature using the conditions included building properties and relevant components such as weather data, a cooling system, infiltration rate, and internal heat gain.

The simulation results in the TRNSYS were transferred to the MATLAB using the Type155 component. The MATLAB software and its neural network toolbox were employed for developing the ANN model and for determining the cooling system operation. Decisions for the cooling system controls based on the ANN prediction result were fed into the TRNSYS in order to operate the cooling system. Then, new simulation results including a new indoor temperature from the TRNSYS were transferred again to the MATLAB. This process was repeated during the simulation period for the data collection and performance tests of the algorithms.

The reliability of the combined method of MATLAB and TRNSYS software was proven in previous studies [45,46], in which the predicted indoor temperatures from an ANN model using the identical method in this study were compared with the measured indoor temperatures from an existing building. The root mean square error (RMSE) between the predicted and measured temperatures was 0.0259 K, smaller than the designated goal of 0.1 K. This finding supports the reliability of the applied simulation method to successfully conduct development and performance tests of an ANN model and control algorithms.

Data sets for the initial model training and correlation analysis were acquired using a test module shown in Fig. 4. The physical properties of the modules are summarized in Table 3. The thermal resistances of the wall, roof, floor and windows of the module were 3.72, 6.80, 3.70, and 0.71 m^2K/W, respectively. A convective cooling system with a heat removal capacity of 10,000 kJ/h was installed for cooling. The ratio of window to wall was 0.20 and 0.10 for the south-facing and north-facing façades, respectively; no windows were installed on the east and west façades. The infiltration rate was assumed to be 2.0 air changes per hour (ACH), a moderate value for a building. Internal heat gain was calculated on the basis of the heat generated by two occupants, equipment and lighting fixtures in space.

The module was assumed to be located in Seoul, South Korea (Latitude: 37.56° N, Longitude: 126.98° E). The data set was collected from June 1 to September 30, which represents typical cooling season in summer. During this period, the weather is hot and humid in Seoul. Typical Meteorological Year (TMY2) weather data were used for the simulations.

One data set represents one day, which means the 100 data sets were acquired throughout 100 days. Normally in Korea, 100 days can make an entire summer season. Thus, 100 days training data sets might be enough to reflect the diverse conditions occurring in the summer.

In addition, the sliding-window method was employed for training data management. Thus, during the iterative training process, the model replaced the oldest data set with the new data set for reflecting the changing environment. Since the developed ANN model conducts the iterative training process with a new data set, the model can adapt itself to the new environment (e.g., change of building orientation) and will produce accurate and stable prediction results.

A minute goal of 0.0, an epoch of 1000 evaluations, a learning rate (LR) of 0.6, and a moment (MO) of 0.2 were initially applied for training based on the optimal values suggested in a previous study [42]. Similar to the N_{HL} and N_{HN}, the optimal number of LR and MO were determined through the optimization process described in Section 2.2.

The linear correlations between the initial input variables (namely, $TEMP_{IN}$, $\Delta TEMP_{IN}$, $TEMP_{OUT}$, $\Delta TEMP_{OUT}$, and $TEMP_{DIF}$)

Table 2
Modeling result and employed TRNSYS types and roles.

Diagram of Modeling Result

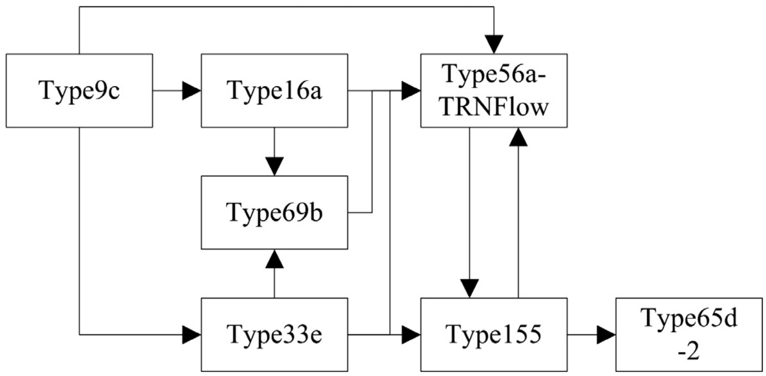

Types and roles		
	Type9c	• Importing a TMY2 weather file for the site
	Type16a	• Calculating solar radiation on building surfaces
	Type33e	• Calculating dew-point temperature of surrounding exterior
	Type69b	• Calculating sky temperature
	Type56a-TRNFlow	• Calling building modeling result of TRNBUILD • Calculating indoor temperature of the test building
	Type155	• Calling the algorithm in MATLAB • Producing training and checking datasets • Calculating signal for the cooling system operation
	Type65d-2	• Producing and displaying the output file

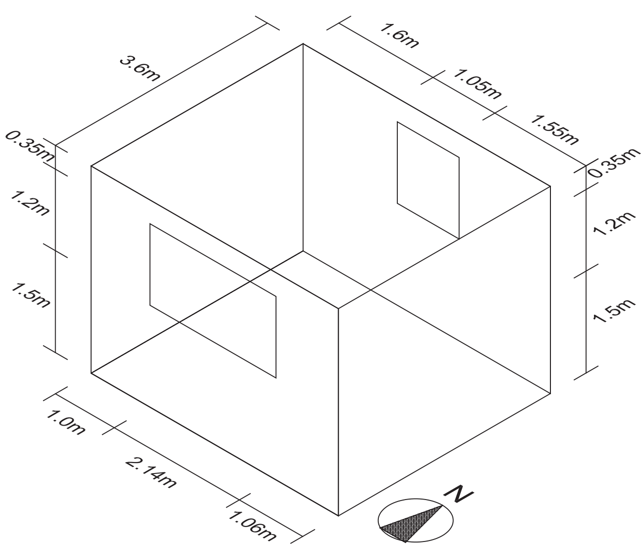

Fig. 4. Structure of tested building for collecting training and checking data sets.

Table 3
Properties of a tested module for collection of datasets used in the ANN model.

Components		Property description
Weather data & climate conditions during cooling season		• TMY2 data for Seoul, South Korea (latitude: 37.56°N, longitude: 126.98°E) • Hot and humid: 23.5 °C air temperature, 72.7% relative humidity from June to September on average
Dimension		– Width: 4.2 m – Depth: 3.6 m – Height: 3.05 m
Envelope insulation [m^2 K/W]		– Exterior wall: 3.72 – Roof: 6.80 – Floor: 3.70 – Window: 0.71 with 6 mm gray glass + 16 mm argon gas + 6 mm gray glass
Cooling system		10,000 kJ/h convective heat removal
Ratio of window to wall		– East: 0.00, – West: 0.00, – South: 0.20, – North: 0.10
Infiltration rate		2.0 ACH
Internal heat gain	Occupants	2 seated-light work persons
	Equipment	2 computers with printer
	Lighting fixtures	5 W/m^2

and the output variable (namely, $TIME_{SBT}$) in one hundred new data sets were statistically analyzed. Data sets were collected identically using the TRNSYS and MATLAB software from the same test building. The input and output variables were used as independent and dependent variables, respectively. Also, the initial ANN model was modified to include only input neurons with strong relevance.

2.2. Optimization

For the purpose of increasing the accuracy and stability of the model, a parametrical optimization process was employed to determine the optimal structure and learning method of the initial ANN model. Several methods for optimizing the structure of the ANN model have been discussed. In some studies, the number of hidden layer and hidden neuron, learning rate, and moment were sequentially tested [22,23,45]. When one parameter (e.g., the number of hidden layer) was tested, other parameters (e.g., the number of hidden layer, learning rate, and moment) were fixed as assigned values.

After finding the optimal value for the first parameter, the second parameter (e.g., the number of hidden neuron) was tested for finding optimal value. At this case, the first parameter was fixed as the found optimal value, and the other two parameters were fixed as assigned values. Then, the identical process was conducted for finding the optimal values for third and fourth parameters (e.g., learning rate and moment).

As an advanced method, the coupled approach for finding optimal structure began to be applied. Two parameters (e.g., the number of hidden layer and neurons) were tested in combination for finding the optimal values together. During this process, the other parameters (e.g., learning rate and moment) were fixed as the assigned values. After found the optimal values for the first two parameters, the last two parameters were tested in the same way [25].

Table 4
Values for optimizing the ANN components.

Parameters to be optimized	Values to be tested
N_{HL}	1, 2, 3, 4, 5
N_{HN}	1, 2, 3, 4, 5, 6, 7, 8, 9, 10
LR	0.1, 0.2, 0.3, 0.4, 0.5, 0.6, 0.7, 0.8, 0.9, 1.0
MO	0.1, 0.2, 0.3, 0.4, 0.5, 0.6, 0.7, 0.8, 0.9, 1.0

In this study, we applied the method that optimizes the parameters in a couple fashion. The optimization was conducted by coupling the ANN parameters: a series of hidden layers (N_{HL}) and hidden neurons (N_{HN}) were tested together, and a series of learning rates (LR) and moments (MO) were tested together. To optimize N_{HL} and N_{HN}, LR and MO were fixed at the initial values (0.6 and 0.2, respectively). Subsequently, LR and MO were optimized by setting N_{HL} and N_{HN} to their optimal values. Table 4 summarizes the parametrical values tested to optimize each parameter.

Another 100 data sets were collected to optimize the model through the method explained in Fig. 4 and Tables 2 and 3 of Section 2.1. The correlations between the numerically simulated values (M_i) using the MATLAB and TRNSYS software and the predicted values (S_i) by ANN model were evaluated. The values that produced the highest coefficients of determination (R^2) for each parameter were determined to be the optimal values.

For evaluating the performance of the optimized models, 100 checking data sets were collected from an identical test module. The precision accuracy was evaluated in terms of the liner correlations between M_i and S_i.

3. Algorithm development and evaluation

One conventional control algorithm and two ANN-based control algorithms were developed to operate the cooling system. The flows of the conventional and ANN-based algorithms are presented in Figs. 5 and 6, respectively. In addition, the descriptions of the three algorithms are summarized in Table 5. The conventional algorithm employs the setback temperature only when $TIME_{CUR}$ is within the setback period. This algorithm is the widespread method for controlling the cooling system.

The ANN-based algorithms employ the setback temperature when the summation of $TIME_{CUR}$ and $TIME_{SBT}$ is at or within the setback period. The ANN-based algorithm I employs the setback operating range when the summation of the current time ($TIME_{CUR}$) and $TIME_{SBT}$ to the lower threshold of the setback operating range is at or after the onset of the setback period. For example, if $TIME_{CUR}$ is 7:30 AM and $TIME_{SBT}$ to 25 °C (the lower threshold of the setback operating range: 25–28 °C) is 30 min, then the algorithm determines to set the setback temperature for the cooling system at this moment because the summation of $TIME_{CUR}$ and $TIME_{SBT}$ reaches the end of the occupied period. Because the cooling system is predictively operated, the indoor temperature increases to the lower threshold of the setback operating range at the moment when the setback is applied. After setback application, this algorithm can considerably reduce the duration of time period, in which the indoor temperature is out of the targeted temperature range.

The ANN-based algorithm II employs setback operating range if the summation of $TIME_{CUR}$ and $TIME_{SBT}$ to the upper threshold of the normal operating range reaches at or after the onset of the setback period. For example, if $TIME_{CUR}$ is 7:20 AM and $TIME_{SBT}$ to the 26 °C, which is the upper threshold of the normal operating range between 23 and 26 °C, is 40 min, then the algorithm determines to set the setback temperature for the cooling system at this moment because the summation of $TIME_{CUR}$ and $TIME_{SBT}$ reaches the end of the occupied period. This algorithm has a probability to keep temperature, which is higher than the targeted range, at the final of the occupied period, but may use less energy than the ANN-based algorithm I.

The temperature conditions using the conventional algorithm and the ANN-based algorithms for the onset of the unoccupied period are shown in Fig. 7. Because the conventional algorithm maintains the normal set-point temperature throughout the occupied period, the indoor temperature is maintained within the normal operating range throughout this period. After the unoccupied period begins, the cooling system begins to increase the temperature to the setback temperature. Thus, cool conditions unnecessarily prevail for a certain period of time after the unoccupied period begins resulting in energy inefficiency.

The thermal and energy performance of the three algorithms were tested according to the procedure described in Fig. 4. Temperature conditions and heat removal by the cooling system were simulated for the cooling season from June 1 to September 30. The layout of a tested building, which was assumed to be a residential building, is shown in Fig. 8. Detailed buildings properties used for performance tests are summarized in Table 6.

The building was assumed to be located in Soul, Korea (Latitude: 37.54° N, Longitude: 126.98° E). For algorithm testing, building characteristics such as dimension, envelope insulation, cooling system capacity, ratio of window to wall, infiltration rate, and internal gain were different from those used in the test model to obtain the training data sets. The dimension of the building was 12.0 m wide, 7.7 m deep and 5.0 m high. The insulation of the wall, roof, floor, and window were 2.84, 5.21, 2.69, and 0.71 m^2K/W of respectively. The heat removal capacity of convective cooling system was 30,000 kJ/h. The ratio of window to wall was 0.14, 0.13, 0.244, and 0.08 for the East, West, South, and North-facing facades, respectively. Infiltration rate was 1.2 air changes per hour (ACH).

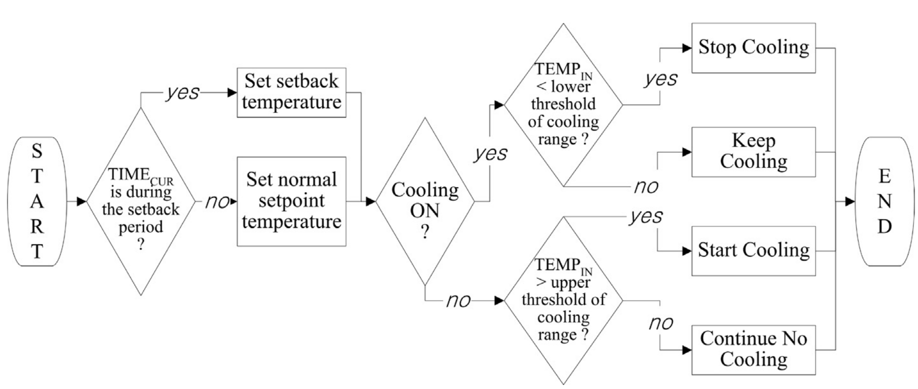

Fig. 5. Flowchart of the conventional algorithm.

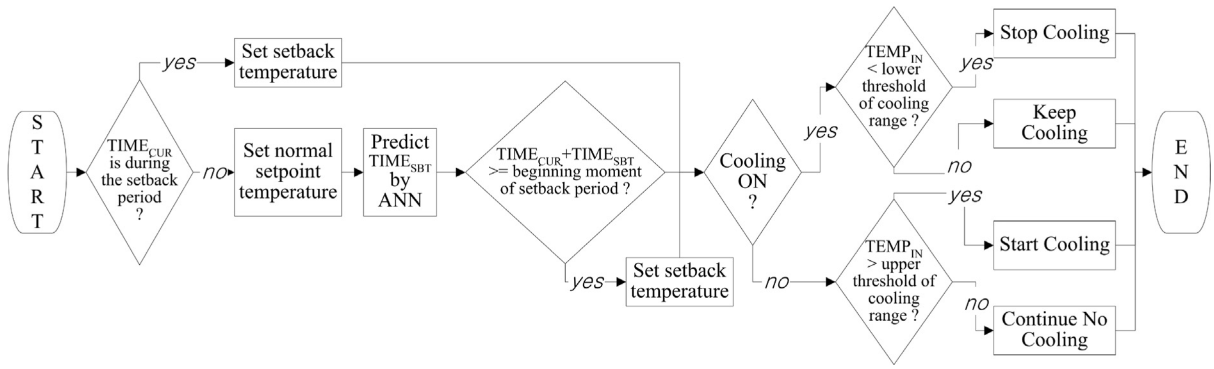

Fig. 6. Flowchart of the ANN-based algorithm.

Table 5
Descriptions of three algorithms.

Algorithms	Principles	
	For occupied period	For unoccupied period
Conventional algorithm	Follow the normal set-point and setback temperature for the occupied and unoccupied period	
ANN-based algorithm I	If $TIME_{CUR} + TIME_{SBT}$ to lower limit of the setback range, then set the setback temperature	Follow the setback temperature for the occupied and unoccupied period
ANN-based algorithm II	If $TIME_{CUR} + TIME_{SBT}$ to upper limit of the normal range, then set the setback temperature	

Four persons, two computers, and lighting fixtures generating 5 W/m^2 were assumed to be the source of internal heat gain.

4. Results

4.1. Development and optimization of the ANN model

Linear regression analysis was performed for input variables (i.e., $TEMP_{IN}$, $\Delta TEMP_{IN}$, $TEMP_{OUT}$, $\Delta TEMP_{OUT}$, and $TEMP_{DIF}$) and output variable (i.e., $TIME_{SBT}$) of the initial model for different setback temperatures from 25.0 °C (setback operating range: 23.5–26.5 °C) to 28.5 °C (setback operating range: 27.0–30.0 °C). For the linear regression, the input variable was used as an independent variable and output variable was used as a dependent variable. The range of $TEMP_{IN}$, $\Delta TEMP_{IN}$, $TEMP_{OUT}$, $\Delta TEMP_{OUT}$, $TEMP_{DIF}$, and $TIME_{SBT}$ of the data sets was 22.20–26.93 °C, −1.49 °C to 1.36 °C, 18.19–29.63 °C, −0.01 °C to 0.03 °C, and 3.07–7.80 °C, and 2–99 min, respectively. Table 7 summarizes the coefficients of determination (R^2) for the linear relationships between the input and output variables.

$TEMP_{IN}$ and $TEMP_{DIF}$ were effectively correlated with $TIMP_{SBT}$. However, the correlations became weaker as the setback temperature was set higher. For the normally recommended setback temperature range of 25.0–26.5 °C, the coefficient of determination (R^2) ranged from 0.4418 to 0.7538. The correlations between $\Delta TEMP_{IN}$, $TEMP_{OUT}$, $\Delta TEMP_{OUT}$ and the output variable were relatively weaker, with R^2 ranging from 0.0030 to 0.2926.

Among all variables, only $TEMP_{IN}$ and $TEMP_{DIF}$ were used as the input variables in the revised ANN model since they correlated with $TIMP_{SBT}$ stronger compared to other variables. Compared to the ANN model which employed three input variables such as $TEMP_{IN}$, $TEMP_{OUT}$, and $TEMP_{DIF}$ for predicting the time duration required for reducing the current indoor temperature to the setback temperature for the heating system in winter [25], $TEMP_{OUT}$ is excluded from the input neurons because the correlation between $TEMP_{OUT}$ and $TIMP_{SBT}$ was weaker in the summer season. It can be inferred that since the outdoor temperature was similar to the setback temperature, $TEMP_{OUT}$ did not significantly impact the amount of $TIMP_{SBT}$.

The structure and learning method of the revised model were optimized using a parametrical process. First, the optimal values for the number of hidden layers (N_{HL}) and the number of hidden neurons (N_{HN}) were determined as values that had the lowest root mean square errors (RMSE) for the difference between the predicted values (S_i) by ANN models and numerically simulated values (M_i) by MATLAB and TRANSYS.

Tables 8 and 9 summarize the root mean square error (RMSE) for the 100 data sets described in Section 2.2. The RMSE for models with 1–5 N_{HL} and 1–10 N_{HN} ranged from 3.14 to 14.53 min as shown in Table 8. The lowest RMSE was obtained when N_{HL} and N_{HN} were set to 1 and 7, respectively. Therefore, the model was optimized by modifying its structure to have 1 hidden layer and 7 hidden neurons. Next, in a similar manner, learning rate (LR) and moment (MO) were optimized by varying these parameters between 0.1 and 1.0 and 0.1 and 1.0, respectively, while setting N_{HL} and N_{HN} to the optimized values.

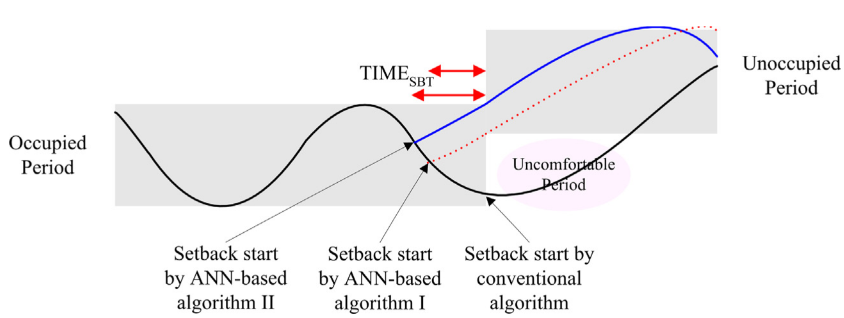

Fig. 7. Comparative temperature conditions by three algorithms.

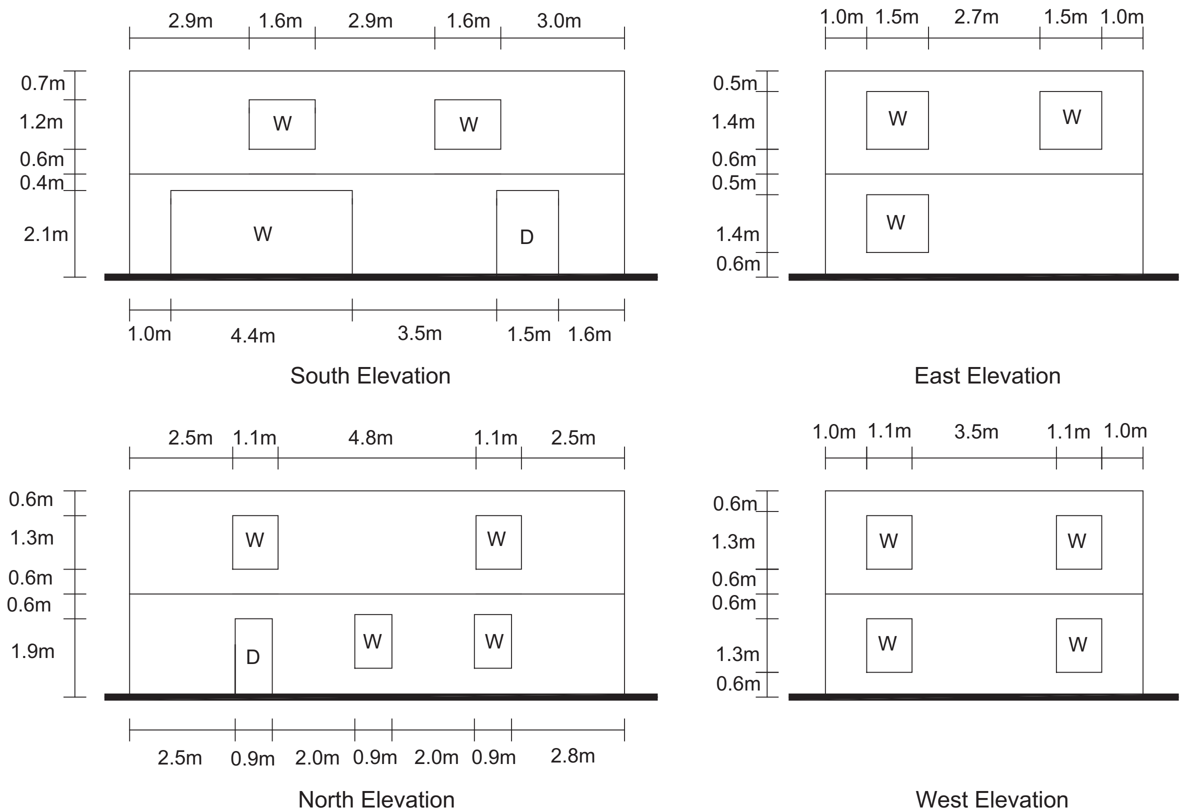

Fig. 8. Layout of a building for performance test (D: Door, W: Window).

Table 6
Features of tested buildings for performance of the algorithms.

Components		Property description
Weather data & climate conditions during the cooling season		• TMY2 data for Seoul, South Korea (latitude: 37.56°N, longitude: 126.98°*E*) • Hot and humid: 23.5 °C air temperature, 72.7% relative humidity from June to September on average
Dimension		– Width: 12.0 m – Depth: 7.7 m – Height: 5.0 m
Envelope insulation [m^2 K/W]		– Exterior wall: 2.84 – Roof: 5.21 – Floor: 2.69 – Window: 0.71 with 6 mm gray glass + 16 mm argon gas + 6 mm gray glass
Cooling system		30,000 kJ/h convective heat removal
Ratio of window to wall		– East: 0.14, – West: 0.13, – South: 0.244, – North : 0.08
Infiltration rate		1.2 ACH
Internal heat gain	Occupants	4 seated- light work persons
	Equipment	2 computers with printer
	Lighting fixtures	5 W/m^2

As shown in Table 9, the lowest RMSE of 2.53 min was obtained when LR and MO were set to 0.6 and 0.7, respectively. Thus, these values were newly applied in the optimized ANN model in Fig. 9, which employed two input neurons ($TEMP_{IN}$ and $TEMP_{DIF}$), 1 N_{HL}, 7 N_{HN}, 0.6 LR, and 0.7 MO. The ANN model which was developed for the heating system in the previous study [25], the optimal values for N_{HL}, N_{HN}, LR, and MO were different to be 4, 9, 0.6, and 0.9. Thus, the respective model needs to be applied for the cooling and heating model.

The linear relationship between predicted values (S_i) by ANN models and numerically simulated values (M_i) by MATLAB and TRANSYS is shown in Fig. 10. The data set used for the regression was based on a prediction phase in order to examine the accuracy of ANN performance in the prediction phase. The linear prediction model between the values is analyzed using the Analysis of Variable (ANOVA), which is a well known test method. The analysis result is summarized in Table 10.

The coefficient of determination (R^2) between the predicted values by ANN models (S_i) and numerically simulated values by MATLAB and TRANSYS (M_i) was 0.9097. Even though R^2 was

Table 7
Coefficient of determination (r^2) between input and output ($TIME_{SBT}$) variables.

Setback temperature (°C)	Input variables				
	$TEMP_{IN}$	$\Delta TEMP_{IN}$	$TEMP_{OUT}$	$\Delta TEMP_{OUT}$	$TEMP_{DIF}$
25.0	0.7538	0.1121	0.0030	0.0779	0.7538
25.5	0.4684	0.2323	0.0208	0.0779	0.4684
26.0	0.6740	0.1708	0.1425	0.1509	0.6740
26.5	0.4418	0.0871	0.0515	0.2926	0.4418
27.0	0.3462	0.0459	0.0630	0.1851	0.3462
27.5	0.3038	0.0077	0.0546	0.1186	0.3038
28.0	0.1996	0.0911	0.0186	0.1837	0.1996
28.5	0.1277	0.0045	0.0848	0.2575	0.1277

Table 8
Root mean square error (RMSE) between S_i and M_i for different N_{HL} and N_{HN}.

		N_{HL}				
		1	2	3	4	5
N_{HN}	1	3.25	3.24	3.25	3.25	3.25
	2	3.64	4.14	3.62	3.99	3.4
	3	3.8	4.09	3.15	3.38	4.1
	4	3.3	4.2	3.39	4.25	3.82
	5	3.43	3.61	3.84	5.99	3.75
	6	3.6	4.45	4.31	7.85	3.69
	7	3.14	5.07	4.79	4.45	5.72
	8	3.42	4.07	4.95	6.03	3.54
	9	3.35	4.25	6.1	7.06	2.67
	10	3.42	5.18	14.53	7	3.82

Table 9
Root mean square error (RMSE) between S_i and M_i for different LR and MO.

		LR									
		0.1	0.2	0.3	0.4	0.5	0.6	0.7	0.8	0.9	1.0
MO	0.1	5.72	3.94	3.2	2.75	3.23	2.8	2.85	2.85	3.45	3.41
	0.2	3.44	3.01	3.45	4.35	2.93	3.13	3.23	3.96	2.96	3.1
	0.3	3.54	4.09	2.92	3.2	2.87	3.24	3.12	3.75	3.91	3.53
	0.4	3.79	3.83	3.7	2.99	3.4	3.21	3.42	3.29	3.48	3.42
	0.5	3.79	3.53	3.88	3.48	3.32	3.16	3.72	3.07	4.33	3.57
	0.6	3.05	3.14	3.03	3.08	4.03	3.01	2.74	3.06	3.66	3.38
	0.7	3.62	3.62	3.67	2.96	3.9	2.53	2.9	2.81	3.19	3.49
	0.8	3.55	3.08	3.67	3.22	3.96	3.42	3.43	3.45	3.54	3.61
	0.9	3.67	3.04	2.98	3.44	3.57	3.6	3.2	3.32	3.98	3.12
	1	3.31	3.39	3.59	3.57	3.74	3.76	3.37	3.76	3.66	3.35

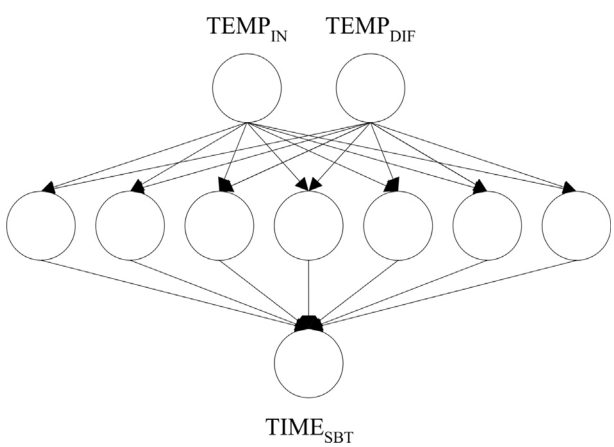

Fig. 9. Optimized ANN model.

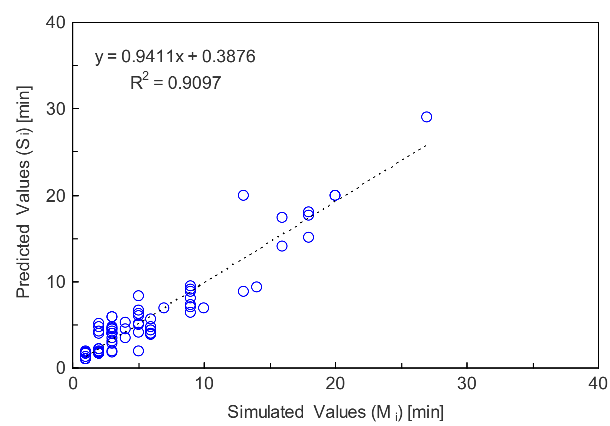

Fig. 10. Relationship between predicted values by ANN models (S_i) and simulated values by MATLAB and TRNSYS (M_i) for the optimized model.

reduced compared to the 0.9999 by the ANN model developed for the heating system [25], the ANVOA test results indicate that the predicted valued by ANN model and the simulated values from the numerical simulation are strongly correlated each other. The prediction model was acceptable under a significance level of 0.01 ($F(98,1) = 987.81$, Sig. = 0.00).

As an additional step to examine the deviation between predicted and simulated values, a frequency analysis was performed. Table 11 shows the difference between the values, root mean square error (RMSE) and coefficient of variation of the room mean square error (CV(RMSE)) between them. The majority of difference was less than 2 min. The RMSE and (CV(RMSE)) between them were 1.57 °C and 31.87%, respectively. Those results imply that the deviation between is within acceptable range. In summary, the prediction accuracy of the ANN model was validated to be applied in the control algorithm.

4.2. Performance of the algorithms

The profiles of the indoor temperature and the cooling system operation for selected three days among all periods used in this study are shown in Fig. 11(a)–(c), when the conventional algorithm, ANN-based algorithm I, and ANN-based algorithm II were applied respectively. Each algorithm operated the cooling system following the set temperatures for the occupied and unoccupied period, respectively. Overall, the indoor temperature were maintained in the designated ranges (23–26 °C for the occupied period and 25–28 °C for the unoccupied period) for most of the time.

For the clear understanding of the difference of the indoor temperature and cooling system operation by three algorithms, Fig. 12 (a)–(c) shows the profiles of the indoor temperature and operation of the cooling system for an extracted period from 7:00 to 9:00 A.M. on August 7. The conventional algorithm, which applied the set-

Table 10
ANOVA test results for linear relationship.

Variables	Unstandardized coefficients		t	Sig.	ANOVA
	B	Std. Error			
(Constant)	0.388	0.21	1.83	0.07	F(98, 1) = 987.81
Simulated value (M_i)	0.941	0.03	31.43	0	Sig. = 0.00, r^2 = 0.9097

Table 11
Frequency analysis and deviation.

Difference range [°C]	0 < X < 1	1 < X < 2	2 < X < 3	3 < X < 4	4 < X < 5	X > 5		
Frequency [%]	24	12	6	2	0	1		
Difference range [°C]	X = 0						RMSE = 1.57 °C	(CV(RMSE)) = 31.81 %
Frequency [%]	11							
Difference range [°C]	−1 < X < 0	−2 < X < −1	−3 < X < −2	−4 < X < −3	−5 < X < −4	X > −5		
Frequency [%]	28	7	5	2	2	0		

back temperature exactly at the onset of the unoccupied period, changed the operating range of the cooling system at 8:00 A.M, following which the cooling system entered the setback operating range (25–28 °C). Thus, the indoor temperature was effectively conditioned between 23 °C and 26 °C during the occupied period. However, the temperature was lower than the lower threshold of the setback operating range for a certain duration after the onset of the unoccupied period, leading to unnecessary energy consumption.

ANN-based algorithms I and II calculated $TIMP_{SBT}$ to 25 °C (lower threshold of the setback operating range) and 26 °C (upper threshold of the normal range) as 2 and 4 min, respectively. Accordingly, the algorithms set the temperature to that within the setback range before the onset of the unoccupied period. Because of this early application of the setback temperature, the cooling system was stopped, and the indoor temperature began to increase in the later part of the occupied period in the morning. The indoor temperature was closer to the target temperature (25 °C and 26 °C for ANN-based algorithms I and II, respectively).

Table 12 summarizes the percentages of time period (PTP), in which the indoor temperature was out of the targeted temperature range, when the indoor temperature was controlled by each control algorithm. During the unoccupied period (8:00 A.M. to 6:00 P.M), the conventional algorithm yielded the largest PTP, but differed non-significantly by only 0.08% and 0.11% when compared with the two ANN-based algorithms.

This insignificant difference is attributable to two reasons. First, the performance over the entire unoccupied period was compared although the performance differed only once, around 8:00 A.M. Thus, these percentages are not truly representative of the performance of the algorithms. Second, the normally recommended setback operating range (25–28 °C) did not differ significantly from the normal operating range (23–26 °C). If this difference was larger, the performance of the algorithms would differ more significantly.

To further clarify the difference among the performance of the algorithms, the PTP in extracted periods of the tests were compared. Fig. 13 depicts the time period (TP) in which the indoor temperature was out of the targeted temperature range, when the indoor temperature was controlled by each control algorithm. The TP was summed for the occupied period (before setback) and unoccupied period (after setback). Test data for days when the indoor temperature was naturally conditioned within the operating range without cooling operation was excluded from the analysis.

Here, the TP before setback is the total duration in which the temperature exceeded 26 °C (upper threshold of the normal operating range) in the last cycle during the occupied period of each day. Similarly, the TP after setback is the total duration in which the temperature was lower than 25 °C (lower threshold of the setback operating range) in the first cycle during the unoccupied period of each day.

During the occupied period, the conventional algorithm did not create any TP in the last cycle of temperature changes. By contrast, ANN-based algorithms I and II generated TP (>26 °C) lasting 3 and 11 min, respectively.

The conventional algorithm and ANN-based algorithms I and II generated TP (<25 °C) lasting 88, 29, and 3 min, respectively. Thus, the total TP (>26 °C and <25 °C) on the analyzed days were 88, 32, and 13 min when the conventional algorithm and ANN-based algorithms I and II were used respectively. These results imply that ANN-based algorithm II, which employs $TIME_{SBT}$ to the upper threshold of the normal range, is the most appropriate to control the indoor temperature within the target range.

The amount of heat removed by the cooling system is summarized in Table 13. During the occupied period (00:00–08:00 A.M.), the conventional algorithm removed the largest amount of heat (789 kW h) from the indoor environment, followed by ANN-based algorithms I (754 kW h) and II (740 kW h). This is because the conventional algorithm maintained the temperature within the normal operating range throughout the occupied period. Compared with the conventional algorithm, the two ANN-based algorithms reduced heat removal by 4.4% and 6.2%.

By contrast, between 08:00 A.M. and 6:00 P.M, the two ANN-based algorithms removed 0.1% and 0.4% more heat than did the conventional algorithm. The total heat removed by the conventional algorithm and ANN-based algorithms I and II were 3102, 3069, and 3063 kW h, respectively.

In general, the amount of heat removal by the cooling system is closely related to the amount of cooling energy consumption. The algorithm which removed more heat from the indoor environment would consume more energy for cooling. Thus, ANN-based algorithm II, which entailed the least heat removal, presented a potential to be the most energy-efficient thermal control algorithm. This reduction in heat removal would be more significant if a higher setback operating range is applied.

5. Conclusion

In this study, prediction models were developed to determine the optimal onset time of the setback temperature of a building during the occupied period in cooling season. Control algorithms employing a prediction model were developed to keep indoor temperature within targeted ranges ensuring energy efficiency. The summary of findings is as follows.

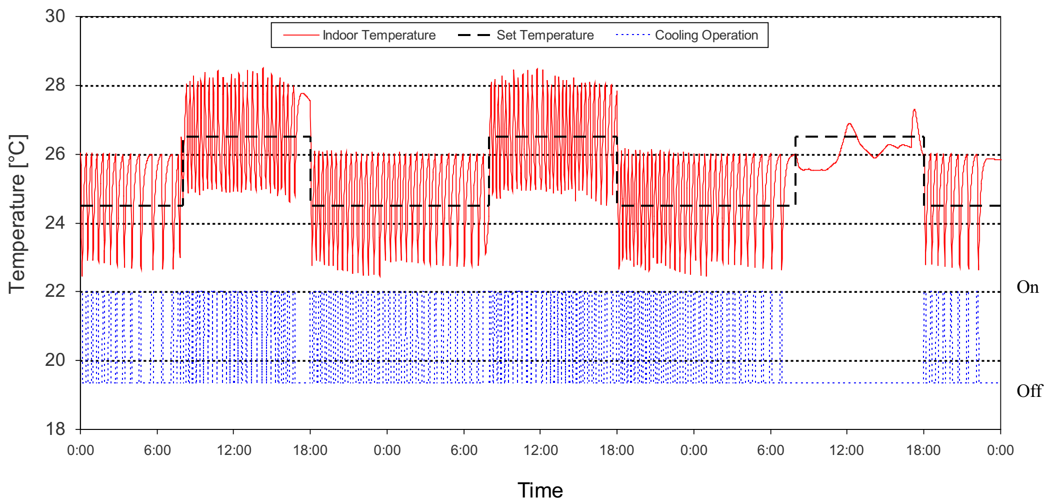

(a) Conventional algorithm

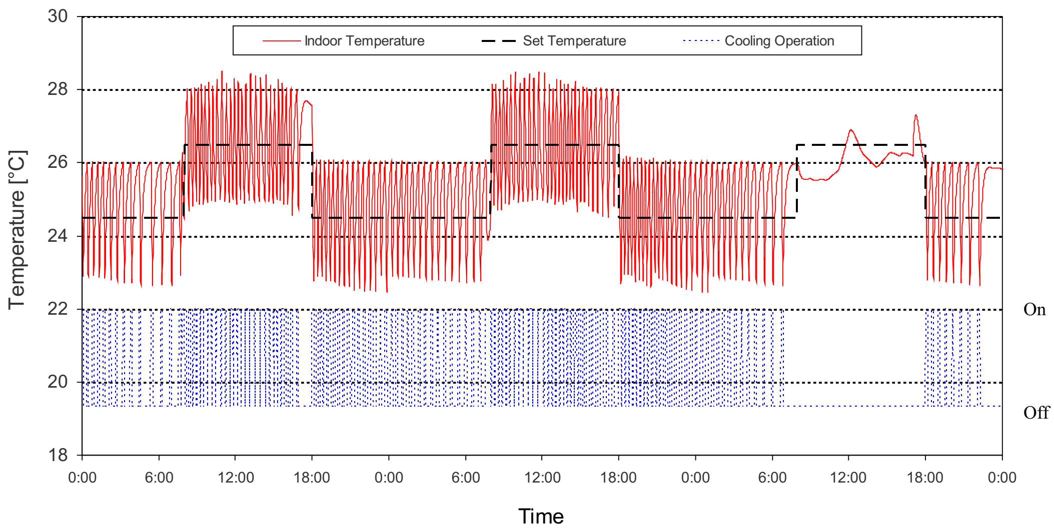

(b) ANN-based algorithm I

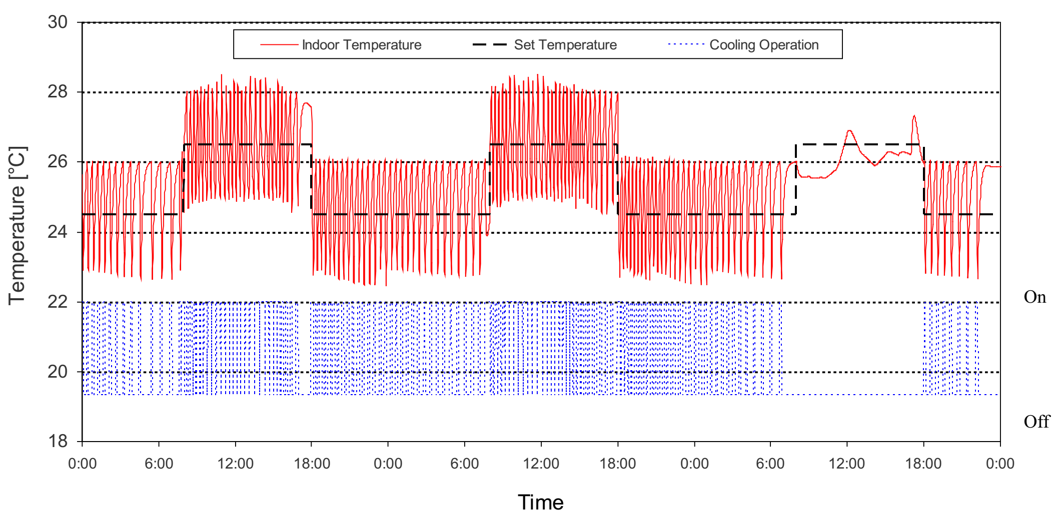

(c) ANN-based algorithm II

Fig. 11. Profile of temperature variation and cooling system operation for selected three days (August 6–August 8).

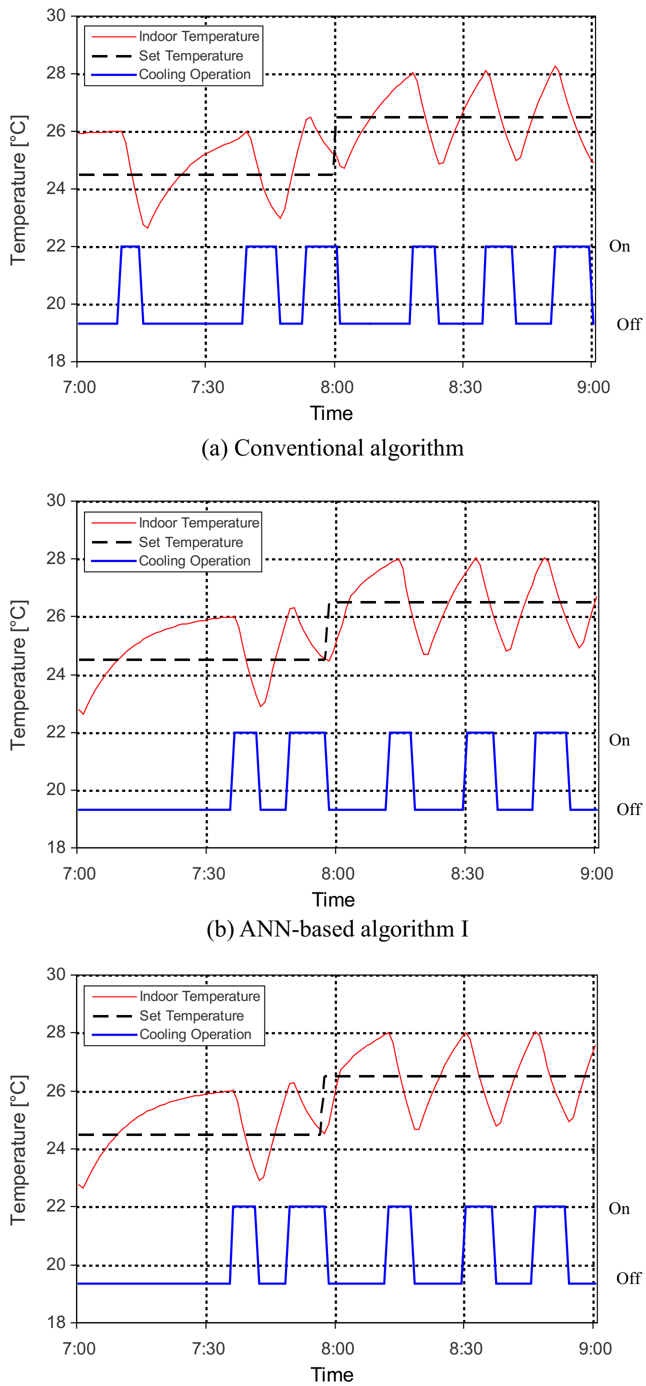

(a) Conventional algorithm

(b) ANN-based algorithm I

(c) ANN-based algorithm II

Fig. 12. Profile of temperature variation and cooling system operation for a extracted period (7:00–9:00 A.M., August 07).

Table 12
Percentages of time period (PTP) that does not meet targeted indoor temperature ranges.

Time	Conventional algorithm [%]	ANN-based algorithm I [%]	ANN-based algorithm II [%]
0:00–8:00	6.59	6.57	7.78
8:00–18:00	9.65	9.57	9.54

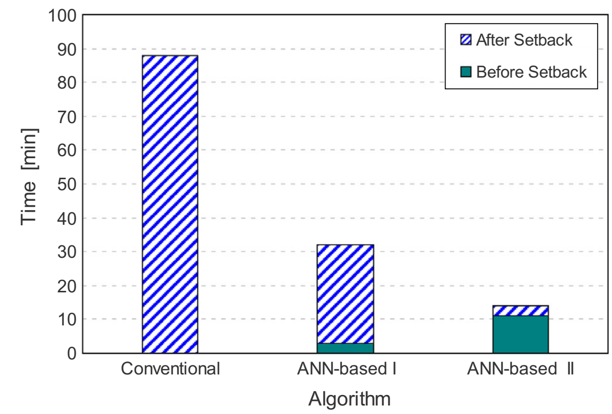

Fig. 13. Time period that does not meet targeted indoor temperature range.

Table 13
Amount of heat removal.

Time	Conventional algorithm [kW h]	ANN-based algorithm I [kW h]	ANN-based algorithm II [kW h]
0:00–8:00	789	754	740
8:00–18:00	2313	2315	2323
Total	3102	3069	3063

(1) Correlation analysis between the input neurons and the output neuron of the initial ANN model revealed strong linear correlations of $TEMP_{IN}$ and $TEMP_{DIF}$ with $TIMP_{SBT}$. Thus, the modified initial ANN model used $TEMP_{IN}$ and $TEMP_{DIF}$ as the input variables.

(2) The RMSE analysis of ANN-model-predicted values and simulated values showed that the optimal number of hidden layers, number of hidden neurons, learning rate, and moment were 1, 7, 0.6, and 0.7, respectively. The optimized ANN model that employed these values had high prediction accuracy ($R^2 > 0.9097$). (Q1-8)

(3) The ANN-based control algorithms could control the indoor temperature within target ranges. Two ANN-based algorithms predictively controlled the cooling system with predetermined setback application. Although the two ANN-based algorithms slightly increased the duration of the time period (TP), in which the indoor temperature was out of the targeted temperature range during occupied periods, they significantly reduced the TP during unoccupied periods. In particular, ANN-based algorithm II, which employs $TIME_{SBT}$ to upper threshold of the normal range, yielded the best performance.

(4) The predictive controls improved the cooling energy efficiency of the building. ANN-based algorithm II effectively reduced the amount of heat removed by the cooling system and was the most energy-efficient thermal control algorithm. If a higher setback operating range is applied, the amount of reduction in heat removal would be more significant.

In this study, the performance of the algorithms was evaluated through one-dimensional (i.e., air temperature within the analysis space and the temperature on each surface were assumed to be uniformly identical) simulations in which limited boundary conditions were applied to an imaginary building. Future studies involving actual field measurements, which can reflect real thermodynamics and air flow, would be useful in validating the applicability of the control algorithm.

Also, further examinations about energy and mass balance should be performed in future studies, since this study provided simple amount of heat removal from space to outdoor environment according to the application of three control algorithms based on the boundary conditions of computer simulations. In order to analyze energy transfer between buildings and outdoor surroundings, theoretical and detailed discussions needs to be provided based on various thermal systems, where energy and mass balance occurred.

Acknowledgements

This research was supported by the Basic Science Research Program through the National Research Foundation of Korea (NRF) funded by the Ministry of Education, Science and Technology (Grant number: 2015R1A1A1A05001142).

References

[1] Ministry of Knowledge Economy, A law for rationalization of energy consumption, Ministry of Knowledge Economy; Available from: <http://www.mke.go.kr>, 2012-05-09.
[2] J.W. Moon, S. Han, Thermostat strategies impact on energy consumption in residential buildings, Energy Build. 43 (2011) 338–346.
[3] L.W. Nelson, Reducing fuel consumption with night setback, ASHRAE J. 15 (1973) 41–49.
[4] A.H. Rosenfeld, Notes on residential fuel use: thermostat and window management, Energy Build. 1 (1977) 99–101.
[5] L.W. Nelson, J.W. MacArthur, Energy savings through thermostat set-back, ASHRAE Trans. 83 (1977) 319–334.
[6] L.W. Nelson, M.A. Ward, Energy savings through thermostat setback, ASHRAE J. 9 (1978) 49–54.
[7] T. Beckey, L.W. Nelson, Field test of energy savings with thermostat setback, ASHRAE J. 23 (1981) 67–70.
[8] J. Ingersoll, J. Huang, Heating energy use management in residential buildings by temperature control, Energy Build. 8 (1985) 27–35.
[9] M.M. Manning, M.C. Swinton, F. Szadkowski, J. Gusdorf, K. Ruest, The effect of thermostat set-back and set-up on seasonal energy consumption, surface temperatures and recovery times at the CCHT Twin House Facility, ASHRAE Trans. 113 (2007) 1–12.
[10] W. McCulloch, W.A. Pitts, Logical calculus of ideas immanent in nervous activity, Bull. Math. Biophys. 5 (1943) 115–133.
[11] J.W. Moon, ANN-based model-free thermal controls for residential building Dissertation for Ph.D., Taubman College of Architecture and Urban Planning, University of Michigan, Ann Arbor, Michigan, USA, 2009.
[12] M. Mohanraj, S. Jayaraj, C. Muraleedharan, Applications of artificial neural networks for thermal analysis of heat exchangers – a review, Int. J. Therm. Sci. 90 (2015) 150–172.
[13] M. Mohanraj, S. Jayaraj, C. Muraleedharan, Applications of artificial neural networks for refrigeration, air-conditioning and heat pump systems – a review, Renewable and Sustainable Energy Reviews 16 (2012) 1340–1358.
[14] L. Mba, P. Meukam, A. Kemajou, Application of artificial neural network for predicting hourly indoor air temperature and relative humidity in modern building in humid region, Energy Build. 121 (2016) 32–42.
[15] S. Papantoniou, D. Kolokotsa, Prediction of outdoor air temperature using neural networks: application in 4 European cities, Energy Build. 114 (2016) 72–79.
[16] C. Deb, L.S. Eang, J. Yang, M. Santamouris, Forecasting diurnal cooling energy load for institutional buildings using Artificial Neural Networks, Energy Build. 121 (2016) 284–297.
[17] Y.T. Chae, R. Horesh, Y. Hwang, Y.M. Lee, Artificial neural network model for forecasting sub-hourly electricity usage in commercial buildings, Energy Build. 111 (2016) 184–194.
[18] K. Li, C. Hu, G. Liu, W. Xue, Building's electricity consumption prediction using optimized artificial neural networks and principal component analysis, Energy Build. 108 (2015) 106–113.
[19] S. Paudel, M. Elmtiri, W.L. Kling, O.L. Corre, Pseudo dynamic transitional modeling of building heating energy demand using artificial neural network, Energy Build. 70 (2015) 81–93.
[20] G. Escrivá-Escrivá, C. Álvarez-Bel, C. Roldán-Blay, M. Alcázar-Ortega, New artificial neural network prediction method for electrical consumption forecasting based on building end-uses, Energy Build. 43 (2011) 3112–3119.
[21] J.W. Moon, Performance of ANN-based predictive and adaptive thermal control methods for disturbances in and around residential buildings, Building and Environment 48 (2011) 15–26.
[22] I.H. Yang, M.S. Yeo, K.W. Kim, Application of artificial neural network to predict the optimal start time for heating system in building, Energy Convers. Manage. 44 (2003) 2791–2809.
[23] I.H. Yang, K.W. Kim, Development of artificial neural network model for the prediction of descending time of room air temperature, Int. J. Air-Cond. Refrig. 12 (2000) 1038–1048.
[24] J.W. Moon, S.K. Jung, Development of a thermal control algorithm using artificial neural network models for improved thermal comfort and energy efficiency in accommodation buildings, Applied Thermal Engineering 103 (2016) 1135–1144.
[25] J.W. Moon, S.K. Jung, Algorithm for optimal application of the setback moment in the heating season using an artificial neural network model, Energy Build. 127 (2016) 859–869.
[26] J.W. Moon, J. Lee, J.D. Chang, S. Kim, Preliminary performance tests on artificial neural network models for opening strategies of double skin envelopes in winter, Energy Build. 75 (2014) 301–311.
[27] S. Kim, J. Lee, J.W. Moon, Performance evaluation of artificial neural network-based variable control logic for double skin enveloped buildings during the heating season, Build. Environ. 82 (2014) 328–338.
[28] J.W. Moon, J. Lee, S. Kim, Application of control logic for optimum indoor thermal environment in buildings with double skin envelope systems, Energy Build. 85 (2014) 59–71.
[29] J.W. Moon, Integrated control of the cooling system and surface openings using the artificial neural networks, Appl. Therm. Eng. 78 (2015) 150–161.
[30] Y.K. Baik, J.W. Moon, Development and performance evaluation of optimal control logics for the two-position- and variable-heating systems in double skin façade buildings, Int. J. Korea Inst. Ecol. Archit. Environ. 14 (2014) 71–77.
[31] A.A. Argiriou, I. Bellas-Velidis, M. Kummert, P. Andre, A neural network controller for hydronic heating systems of solar buildings, Neural Network 17 (2004) 424–440.
[32] A.A. Argiriou, I. Bellas-Velidis, C.A. Balaras, Development of a neural network heating controller for solar buildings, Neural Network 13 (2000) 811–820.
[33] N. Morel, M. Bauer, M. El-Khoury, J. Krauss, NEUROBAT, a predictive and adaptive heating control system using artificial neural networks, Int. J. Sol. Energy 21 (2001) 161–201.
[34] J.Y. Lee, M.S. Yeo, K.W. Kim, Predictive control of the radiant floor heating system in apartment buildings, J. Asian Archit. Build. Eng. 1 (2002) 105–112.
[35] J.Y. Lee, I.H. Yang, S.Y. Song, H.S. Kim, K.W. Kim, A study of the predictive control of the ondol system in apartments, in: Proceedings of the International Building Performance Simulation Association, Kyoto (Japan), 1999, pp. 215–222.
[36] W. Yaïci, E. Entchev, Performance prediction of a solar thermal energy system using artificial neural networks, Appl. Therm. Eng. 73 (2014) 1348–1359.
[37] T.T. Chow, Z. Lin, C.L. Song, G.Q. Zhang, Applying neural network and genetic algorithm in chiller system optimization, in: Proceedings of the Seventh International Building Performance Simulation Association, Rio De Janeiro (Brazil), 2001, pp. 1059–1065.
[38] H. Esen, M. Inalli, A. Sengur, M. Esen, Forecasting of a ground-coupled heat pump performance using neural networks with statistical data weighting pre-processing, Int. J. Therm. Sci. 47 (2008) 431–441.
[39] H. Esen, M. Inalli, A. Sengur, M. Esen, Artificial neural networks and adaptive neuro-fuzzy assessments for ground-coupled heat pump system, Energy Build. 40 (2008) 1074–1083.
[40] H. Esen, M. Inalli, A. Sengur, M. Esen, Performance prediction of a ground-coupled heat pump system using artificial neural networks, Expert Syst. Appl. 35 (2008) 1940–1948.
[41] J.C. Fannou, C. Rousseau, L. Lamarche, S. Kajl, Modeling of a direct expansion geothermal heat pump using artificial neural networks, Energy Build. 81 (2014) 381–390.
[42] J.W. Moon, K. Kim, H. Min, ANN-based prediction and optimization of cooling system in hotel rooms, Energies 8 (2015) 10775–10795.
[43] MathWorks, MATLAB 14, vol. 26; Available from: <http://www.mathworks.com>; 2014-10. p. 10-17.
[44] University of Wisconsin, TRNSYS16.1; Available from: <http://sel.me.wisc.edu/trnsys/>; 2014-10.
[45] J.W. Moon, S.H. Yoon, S. Kim, Development of an artificial neural network model based thermal control logic for double skin envelopes in winter, Build. Environ. 61 (2013) 149–159.
[46] J.W. Moon, J.D. Chang, S. Kim, Artificial neural network for controlling the openings of double skin envelopes and cooling systems, in: Proceedings of the 2012 International Conference on Sustainable Design and Construction, Fort Worth (USA), 2012, pp. 81–89.